

# Display Forming Polymer/Liquid Crystal Composite Layers and Their Stability Against External Mechanical Distortions

M. Bauer,<sup>1</sup> L. Hartmann,<sup>1</sup> F. Kuschel,<sup>1</sup> B. Seiler,<sup>2</sup> E. Noack<sup>2</sup>

<sup>1</sup>Fraunhofer Research Institution for Polymeric Materials and Composites PYCO, Teltow D-14513, Germany

<sup>2</sup>Chemnitz Materials Mechanics Ltd., Chemnitz D-09117, Germany

Received 7 April 2009; accepted 22 January 2010

DOI 10.1002/app.32140

Published online 1 April 2010 in Wiley InterScience (www.interscience.wiley.com).

**ABSTRACT:** The liquid crystal display (LCD) technology is confronted with the task to substitute rigid glass plates enclosing the electro-optically active liquid crystal (LC) material by plastic substrates. In particular, the commercialization of flexible displays requires a sufficient stabilization against external mechanical distortions. To achieve LC layer stabilization, several procedures have been suggested. In this work, the thermal-induced phase separation (TIPS) technique has been applied to generate composite films consisting of LC compartments which are encased by coherent polymer walls after binodal phase separation. Composite films were prepared from a series of poly(methacrylates) and various commercial nematic LC mixtures. Furthermore, the use of copolymers as well as binary blends from “hard” and “soft” poly(methacrylates) broadens the possibilities to control the film morphology. To compare different polymer/LC composite films regarding

their stability under compression load, the samples were investigated by indentation tests using an inverse reflected-light microscope combined with a digital image acquisition technique. The deformation of the composite layers was evaluated by the *uniDAC* image analysis which relies on the more general method of Digital Image Correlation (DIC). Some of the fabricated composites show a remarkably high indentation resistance, especially such prepared from poly(1-tetralyl methacrylate) and poly(4-*tert*-butylcyclohexyl methacrylate). The results facilitate the selection of suitable composite systems for the fabrication of mechanically stabilized flexible LC displays. © 2010 Wiley Periodicals, Inc. *J Appl Polym Sci* 117: 1924–1933, 2010

**Key words:** polymer/LC composites; phase separation; LC compartments; morphology; mechanical properties

## INTRODUCTION

The morphology and phase behavior of blends prepared from liquid crystals and polymers are strongly determined by the chemical constitution, molecular structure, and concentration of the components.<sup>1,2</sup> Whereas a low contents of thermoplastic polymers results usually in homogeneous solutions characterized by network morphology, higher concentrations lead to segregation and the formation of LC- or polymer-compartments. With respect to composition, extension, coherency, and structure, these compartments may be strongly different depending on the mutual miscibility and the separation procedure. A large number of studies have emphasized the phase behavior and thermodynamic aspects of polymer/LC blends accompanied by efforts toward getting the theoretical basis to interpret the experimental results.<sup>3</sup>

Considerable attention has been paid to LC-polymer mixtures for electro-optical applications.<sup>4</sup> Depending on the phase structure,<sup>5</sup> different types of blends used in display systems have been designated as follows:

- Polymer-stabilized liquid crystals (PSLCs), if relatively small amounts of molecular dispersed polymers are solved in low-molecular weight LC phases,<sup>6</sup>
- Polymer-dispersed liquid crystals (PDLCs), characterized by a biphasic structure consisting of separated LC compartments distributed in a polymer matrix,<sup>7,8</sup>
- Liquid crystal dispersed polymers (LCDPs) exhibiting polymer aggregates, e.g., polymer balls, distributed in a coherent LC host phase.<sup>9</sup>

The size, shape, distribution, and director orientation of LC subphases in PDLCs may be adjusted to the intended electro-optical application. In most PDLCs, the size of droplet-like LC particles is comparable to the wavelength of ambient light, i.e., the thickness of the PDLC device is much larger than the LC domain size.

Correspondence to: M. Bauer (monika.bauer@pyco.fraunhofer.de).

Another situation occurs, if composite layers with relatively low contents of polymers are used and the size of the separated LC domains exceeds the layer thickness. Provided that the LC domains are isolated and the polymer forms a coherent wall pattern, the electro-optical behavior of the LC is nearly independent on the morphology. These polymer matrix layers can be used to stabilize the cell gap of LC devices. They are of interest, because one of several problems connected with the LCD panel manufacturing using plastic substrates is a reliable cell gap control technique. To realize LCD layer stabilization, a large number of patterning procedures has been suggested.<sup>10</sup> Besides of preassembly methods, e.g., photolithography, inkjet printing, and emulsification,<sup>11</sup> several postfilling techniques may be applied as follows:

- Generation of a supporting structure exhibiting different morphologies (networks or fibers) by delocalized polymerization-induced phase separation (PIPS),
- Formation of walls in the interpixel region of the substrates using photopolymerization,<sup>12</sup> also in presence of an electric field<sup>13</sup> or induced on patterned polyimide films,<sup>14</sup>
- Solvent-induced phase separation (SIPS) or thermally induced phase separation (TIPS) may produce a coherent solid polymer scaffold which surrounds the insulated LC domains.

Apart from the problem of cell gap controlling, such encapsulation prevents (i) material flow under display flexing and bending and (ii) the intermixing of LC domains after a pinpointed pretreatment for generation of different colors by photochemical tuning.<sup>15</sup> Because complete segregation of monomers or UV curable material during the PIPS process is hard to achieve, this publication will only deal with composites generated by TIPS using selected polymers.

Several studies investigating such TIPS composites have been published, e.g., poly(vinyl butyral) (PVB)/ZLI-2806,<sup>16</sup> polystyrene (PS)/E7,<sup>17</sup> poly(methyl methacrylate) (PMMA)/E7,<sup>18-20</sup> poly(*n*-butyl methacrylate) (PBMA)/E7,<sup>19</sup> PMMA/E8,<sup>21</sup> poly(*n*-butyl acrylate) (PBA)/E7,<sup>22</sup> poly(2-hydroxyethyl methacrylate) (PHEMA), PMMA, poly(vinyl chloride) (PVC)/three single LC compounds.<sup>23</sup> In these papers, the phase diagrams of LC/polymer systems, the separation mechanisms, the morphologies of the composite films, and the electro-optical properties have been mainly investigated. However, with respect to cell gap stabilization and reliable LC encapsulation in displays fabricated with plastic substrates and different LC mixtures, the necessity to explore new material combinations exhibiting improved LC compartmentalization is recognized.

In this study, the fabrication, the morphological, and mechanical properties of composite films with isolated LC compartments made from frequently used commercial nematic LC mixtures and different poly(methacrylates) bearing alkyl or cycloalkyl substituents is reported. The composites were obtained by binodal thermally induced phase separation. Because stability against mechanical distortions is an essential requirement for an undisturbed operation of devices, indentation tests on polymer/LC composite layers with varying composition have been performed.

## EXPERIMENTAL

### Materials and characterization

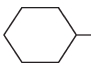
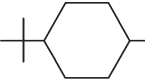

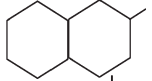
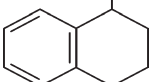
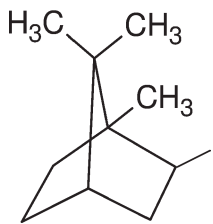
The nematic multicomponent LC-mixtures used in these experiments were L101 (home made), E7, MDA-00-1795, MLC-6650 (Merck), and ZOC-1002XX (Chisso Co.). L101 exhibits a nematic-isotropic temperature  $T_{ni}$  of 60°C and contains 39.1 wt % 4-pentyl-4'-cyanobiphenyl, 24.7 wt % 4-heptyl-4'-cyanobiphenyl, 13.3 wt % 4-octyl-4'-cyanobiphenyl, 9.1 wt % 4-pentyl-4'-cyanoterphenyl, 8.6 wt % 4-butylbenzoic acid-4'-cyanophenylester, 3.4 wt % 4-heptylbenzoic acid-4'-cyanophenylester, and 1.7 wt % 4-pentylbenzoic acid-4'-cyanophenylester.

As homopolymer matrices were used poly(methyl methacrylate) (PMMA,  $M_n = 15,000; 120,000; 350,000; 996,000 \text{ g mol}^{-1}$ ) and poly(ethyl methacrylate) (PEMA,  $M_n = 45,000 \text{ g mol}^{-1}$ ) from Aldrich/Germany as well as own synthesized poly(cycloalkyl methacrylates): poly(cyclohexyl methacrylate) (PCHMA), poly(4-*tert*-butylcyclohexyl methacrylate) (PTBMA), poly(4-cyclohexylcyclohexyl methacrylate) (PBCHMA), poly(decahydro-2-naphthyl methacrylate) (PDHNMA), poly(1-tetralyl methacrylate) (PTMA), and poly(isobornyl methacrylate)(PIBMA), respectively. For chemical structure and properties of the latter see Table I.

Besides homopolymers, two copolymers were synthesized: poly(cyclohexyl methacrylate-*co*-isobornyl methacrylate) [P(CHMA-*co*-IBMA)] and poly(cyclohexyl methacrylate-*co*-adamantanyl methacrylate) [P(CHMA-*co*-ADMA)]. For chemical structure, composition and further properties see Table II.

Monomers CHMA and IBMA were supplied from Aldrich and purified by distillation under reduced pressure. TBCHMA was obtained by conversion of 4-*tert*-butyl-cyclohexanol (mixture of isomers, TCI), dissolved in ethyl methyl ketone, with methacryloyl chloride in the presence of triethylamine. BCHMA, DHNMA, TMA, and ADMA were prepared in a similar manner from commercial 4-cyclohexylcyclohexanol (TCI), 2-decahydronaphthol (a mixture of four isomers), ( $\pm$ )-1,2,3,4-tetrahydro-1-naphthol, and 1-adamantanol (all from Aldrich) by esterification

TABLE I  
Chemical Structure and Properties of Matrix Homopolymers

Basic polymer structure		$\left[ \text{CH}_2 - \underset{\text{COOR}}{\text{C}}(\text{CH}_3) \right]_n$		
Code	R	$M_n$ (g mol <sup>-1</sup> )	PDI	$T_g$ (°C)
PCHMA		38,000	3.8	105 <sup>a</sup> , 83 <sup>24</sup>
PTBCHMA		16,500	2.7	151 <sup>a</sup> , 178 <sup>25</sup>
PBCHMA		9,000	1.9	127 <sup>a</sup>
PDHNMA		10,800	2.4	143 <sup>a</sup> , 145 <sup>24</sup>
PTMA		11,500	2.2	118 <sup>a</sup>
PIBMA		19,000	2.5	167 <sup>a</sup> , 123 <sup>24</sup>

PDI, polydispersity index;  $T_g$ , glass transition temperature.

<sup>a</sup> This work.

with methacryloyl chloride. Except for ADMA, the monomers were distilled under reduced pressure for purification (TBCHMA bp ca. 77°C/0.5 mm, BCHMA bp ca. 95°C/0.5 mm, DHNMA bp ca. 85°C/1 mm, TMA bp 92–96°C/0.5 mm). ADMA was purified by column chromatography on silica gel with toluene as eluent.

PMMA and PEMA were used as received. PCHMA, PTBCHMA, PBCHMA, PDHNMA, PTMA, and PIBMA, respectively, were obtained by polymerization of the corresponding monomers in xylene (mixture of isomers) in the presence of AIBN in Schlenk tubes at 60°C. After 15 h, the polymers were precipitated in methanol and purified by repeated reprecipitation with methanol from solution in chloroform followed by drying in vacuum. Copolymers were obtained from predetermined quantities of CHMA, IBMA, and ADMA in the same procedure as described for homopolymers.

Monomeric methacrylates were characterized by analytical thin-layer chromatography using SIL G/UV254 plates (Machery-Nagel/Germany) and UV or

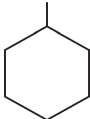
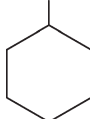
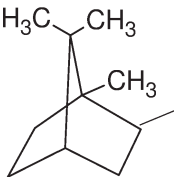
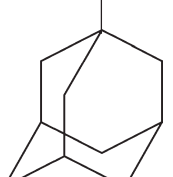
$I_2$  visualization. <sup>1</sup>H- and <sup>13</sup>C-NMR spectra were recorded on a Unityplus-300 QNP or Varian Gemini 2000 (400 MHz). GPC measurements were performed in THF at 25°C by means of the Jasco PU 1585 system with Phenogel 300 × 7.8 mm ID (50 Å, 100 Å, and 1000 Å) columns. The number average molecular weights  $M_n$  were calibrated with standard polystyrenes. Glass transition temperatures were determined using a Mettler Toledo DSC 821<sup>e</sup> with a heating rate of 5 K/min.

### Preparation of composite films

Phase separated composite films were prepared by the TIPS method using three different cell versions:

- To study the basic phase behavior (miscibility, separation, and morphology) glass cells of about 1 cm × 1 cm area and with a gap of about 6 μm were used.
- Composite films were also prepared in a 3.5 μm thin gap between two indium-tin-oxide-coated PET sheets (ITO/PET) with a thickness of 180 μm.

TABLE II  
Chemical Structure and Properties of Matrix Copolymers

Basic polymer structure	$\left[ \text{CH}_2 - \underset{\text{COOR}_1}{\text{CH}(\text{CH}_3)} \right]_x \cdots \left[ \text{CH}_2 - \underset{\text{COOR}_2}{\text{CH}(\text{CH}_3)} \right]_y$	
	P(CHMA-co-IBMA)	P(CHMA-co-ADMA)
R <sub>1</sub>		
R <sub>2</sub>		
x <sup>a</sup>	0.5	0.66
y <sup>a</sup>	0.5	0.34
M <sub>n</sub> (g mol <sup>-1</sup> )	23,000	33,000
PDI	2.5	1.8
T <sub>g</sub> (°C)	127	130

<sup>a</sup> Initial ratio of monomers.

C. Spacerless hybrid cells consisting of a supporting glass substrate and a 180- $\mu\text{m}$  thick covering ITO/PET foil have been used for indentation tests. The average thickness of the cell gap was 10  $\mu\text{m}$ .

The gap of type A and B cells was adjusted using mineral mounting spacers. Cell filling has been performed in the following manner: A homogeneous solution of the LC and the polymer diluted in chloroform was filled in a small glass container. After complete removal of the solvent by slow evaporation, the inhomogeneous residue was heated up to 120°C to form an isotropic solution. A small amount of the isotropic solution was transferred to the filling hole of a heated empty cell (type A or B) using a heated stainless steel tip. The filling took place by capillary forces. Filled cells of type C were prepared according to the one-drop-filling technique by placing the ITO/PET foil on top of the supporting glass substrate bearing a mixture droplet of about 1  $\mu\text{L}$  at 120°C.

Upon complete filling, the cells have been kept for 10 min at 120°C and — if not stated otherwise — subsequently cooled to room temperature at a rate of 1 K/min.

#### Microscopic observations

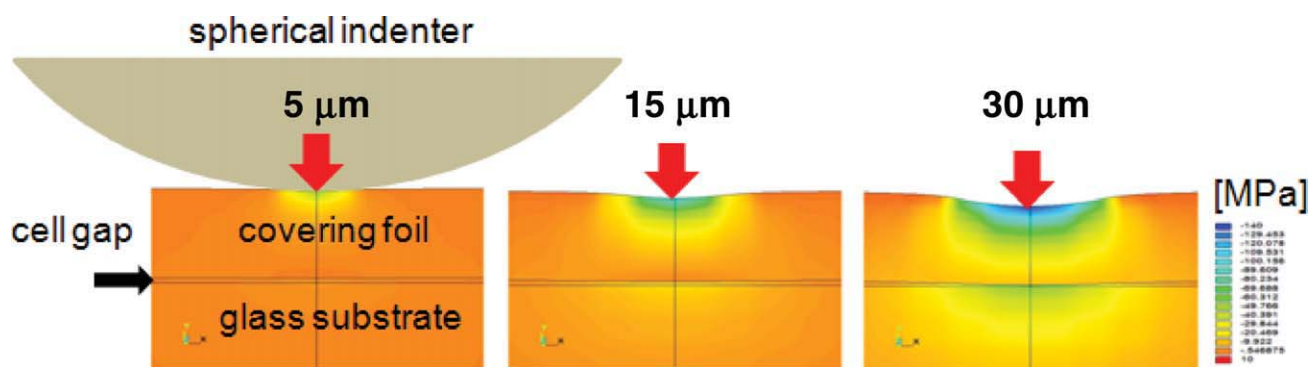
The samples were placed on a home made calibrated hot stage of a Nikon Labophot 2 polarizing optical

microscope (POM) to explore the phase separation processes, the resulting textures and overall morphologies, especially the size, shape, and distribution of LC domains as well as the coherency of the surrounding polymer matrix. Texture images were captured at room temperature.

#### Indentation tests

Comparative indentation tests were performed with type C cells by using a measurement setup consisting of an inverse reflected-light microscope, digital image acquisition, and indentation equipment with a spherical indenter of 1 mm diameter. Before the measurement, Finite Element Method simulations have been performed to investigate qualitatively if an indentation of up to 80  $\mu\text{m}$  is sufficient to create representative deformations of the cell gap. For this simplified linear elastic simulation, estimated material parameters were used, but compliances of the setup were not considered. Results of this simulation as well as the measurement geometry are given in Figure 1.

The loading of cells up to an indentation depth of 80  $\mu\text{m}$  was performed in steps of 1  $\mu\text{m}$  controlled by a linear actuator having a resolution of 1  $\mu\text{m}$  in the measurement range up to 100  $\mu\text{m}$ . Forces acting on the sample cell were recorded by a load cell KAP-S,



**Figure 1** Hydrostatic pressure simulated by FEM for indicated values of the indentation depth into the covering foil of type C cells. It serves as a measure for the intensity of compression loading in the cell gap. [Color figure can be viewed in the online issue, which is available at [www.interscience.wiley.com](http://www.interscience.wiley.com).]

with a resolution of 0.1 N in the measurement range up to 200 N, which was mounted on top of the indenter. The conditions of the sample cells were analyzed by digital image acquisition. Images of  $3 \times 2$  mm of the sample were acquired at values of the indentation depth between  $5 \mu\text{m}$  and  $80 \mu\text{m}$  with an increment of  $5 \mu\text{m}$ . Besides this selected test procedure, a higher indentation depth has been applied on the most resistant material compound to evaluate the behavior regarding higher stresses (cf. Fig. 7).

To quantify the impact of the deformation on the constitution of the LC-filled polymer compartments, the image correlation method *uniDAC* (Universal Deformation Analysis by Correlation)<sup>26,27</sup> has been applied, a special proprietary development based on the Digital Image Correlation (DIC). In doing so, a picture of the sample cell under load together with a picture of the unstressed cell as reference are subjected to a two-dimensional cross correlation analysis. This analysis is applied consecutively to local gray scale matrices taken from both images in the vicinity of predefined points of measurement. The so obtained maximum cross correlation coefficient serves as a measure for the local deformation of the composite with respect to the unloaded state. It allows for comparing the area of efficacy resulting from compression load for different composite films. The lateral resolution is improved by using an additional subpixel algorithm.

The determination of the correlation coefficient allows comparing cells filled with different polymer/LC composites with regard to their indentation resistance. For this purpose, the correlation coefficient has been visualized in the digitized color images as measure for the degree of the cell damages. Green areas (correlation coefficient of  $\sim 1$ ) are unaffected by the indentation, in red areas, the indentation test has the strongest impact on the polymer/LC composite cells (cf. Figs. 6–8).

## RESULTS AND DISCUSSION

### Evaluation of matrix polymers

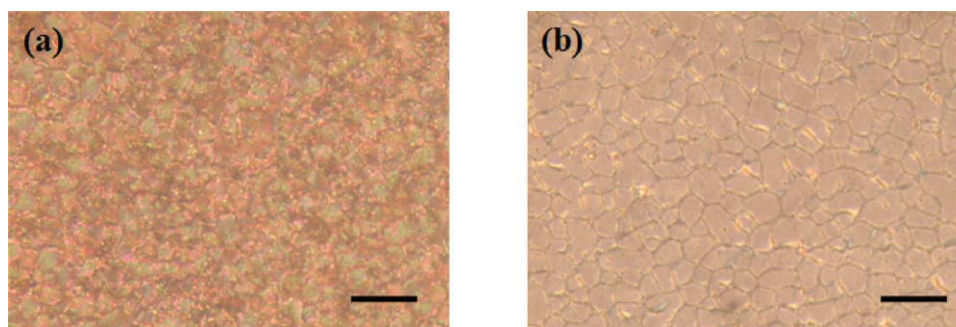
To limit the number of polymer/LC combinations used in further investigations, the mixing behavior and phase separation of all polymers with the nematic mixture L101 as host system have been evaluated using cells of type A. All composite samples contain 20 wt % of the polymer. The results are given in Table III.

These tests revealed that miscibility at a temperature above the clearing point of the pure LC material ( $120^\circ\text{C}$  in this study) is an indispensable but not sufficient condition for the formation of a clearly defined droplet structure in the diphasic region. Obviously, there are two border cases:

- If the phase separation coming from the single phase regime by cooling is delayed, spinodal decomposition accompanied by an

**TABLE III**  
Optical Properties and Morphology of Composites Containing 80 wt % L101

Polymer	Light transmission of the melt at $120^\circ\text{C}$	Composite layer (room temperature)
PMMA 350,000	turbid	unspecific textures, continuously interpenetrating phases
PMMA 996,000		
PBCHMA		
PIBMA		
P(CHMA-co-ADMA)	clear	
PMMA 15,000		
PMMA 120,000		
PEMA	clear	LC droplets embedded in a coherent polymer phase
PCHMA		
PTBCHMA		
PDHNMA		
PTMA		
P(CHMA-co-IBMA)		



**Figure 2** Polarizing optical microscope (POM) images (parallel polarizers) of LC/polymer composite morphologies for PMMA 120,000/L101 (10.4/89.6 wt %) in cell type A after cooling from 100°C to room temperature with 1 K/min. The images were captured at different distances from the filling edge: (a) 5 mm and (b) 15 mm. The mean lateral dimension of the LC-filled compartments in (b) is 12 μm. Scale bars indicate 25 μm. [Color figure can be viewed in the online issue, which is available at [www.interscience.wiley.com](http://www.interscience.wiley.com).]

interconnected two-phase morphology occurs. Such behavior can be observed preferably with components exhibiting a relatively large difference between clearing temperature  $T_{ni}$  of the LC and  $T_g$  of the polymer.

- A metastable state is formed which allows nucleation and growth leading to the formation of polymer-rich and LC-rich isolated phases by binodal decomposition. Components with a relatively low difference between  $T_{ni}$  and  $T_g$  are candidates for this kind of pattern formation.

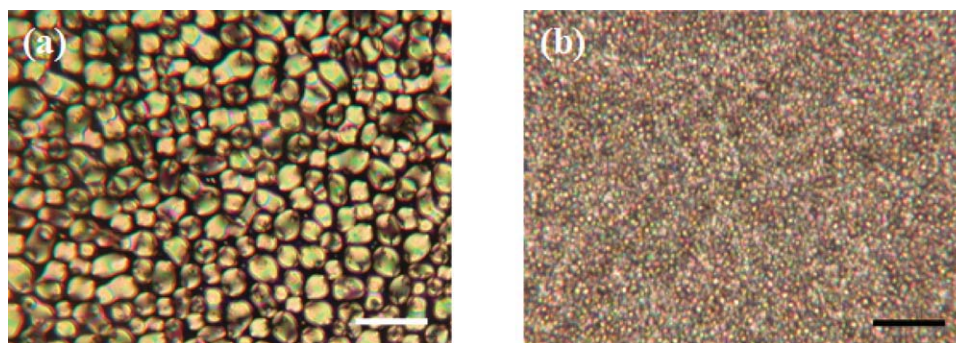
However, in such phase separated systems, an enhanced mutual solubility of the components is often found restricting the practical applicability for PDLC<sup>19</sup> and also for mechanical layer stabilization. The temperature difference  $T_g - T_{ni}$  does not determine exclusively the mutual solubility of the components. Therefore, it is necessary to find appropriate polymers and mixture ratios which allow the formation of stable LC droplet structures by binodal decomposition for each individual case. As example, optical micrographs of various film morphologies

using polarized light for illumination are shown in Figures 2–5.

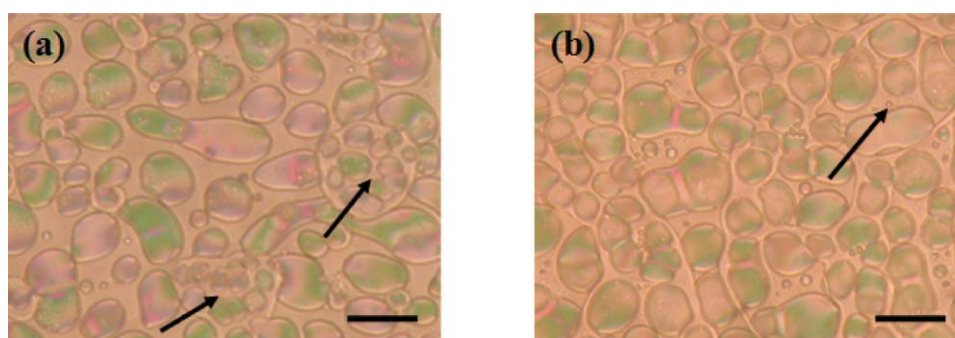
### Morphological features

Probably because of partial phase separation at about 120°C followed by spinodal decomposition mode, cells with PMMA/L101 composite films featured nonuniform constitution and textures depending on the distance from the filling edge. At low distances (about 5 mm), a less organized morphology without distinct domains occurred [Fig. 2(a)]. This figure corresponds to results obtained for PMMA/E7<sup>19</sup> and PS/E7.<sup>17</sup> At a distance of about 15 mm, the texture may be regarded as an inverse structure which is dominated by polymer-rich islands separated by LC-rich thin gaps [Fig. 2(b)].

After substitution of PMMA by PCHMA, a uniform cellular composite morphology with a distinct dependence of the LC domain sizes on the thermal history appeared. This dependence on the cooling regime starting at the homogeneous mixture is exemplified by PCHMA/L101 in Figure 3. A cooling rate of 1 K/min after the onset of phase separation



**Figure 3** Composite layers after different cooling rates: PCHMA/L101 (17.9/82.1 wt %) in cell type A was cooled from 120°C to room temperature at (a) 0.1 K/min and (b) 10 K/min. The mean lateral dimension of the LC-filled compartments is 10 μm in (a) and 3 μm in (b). Images were captured with crossed polarizers, scale bars indicate 25 μm. [Color figure can be viewed in the online issue, which is available at [www.interscience.wiley.com](http://www.interscience.wiley.com).]



**Figure 4** POM images (parallel polarizers) of three-phase composite layers (PDHNMA/PEMA/ZOC-1002XX) in cell type A after cooling from 120°C to room temperature with 1 K/min: (a) 18/2.9/79.1 wt % and (b) 15/5/80 wt %. Arrows indicate separated composite domains formed by the minor polymer component, PEMA. Scale bars indicate 25  $\mu\text{m}$ . [Color figure can be viewed in the online issue, which is available at [www.interscience.wiley.com](http://www.interscience.wiley.com).]

ensures the generation of LC droplets with an optimal size between 5  $\mu\text{m}$  and 20  $\mu\text{m}$ . In this case, bright LC domains are surrounded by dark polymer walls after complete phase separation [Fig. 3(a)]. Nonoptimal cooling hinders complete phase separation and leads to LC domains being too small for display applications [Fig. 3(b)].

From practical reasons, it could be of interest to achieve a partial flexibility of a rigid polymer/LC composite scaffold by incorporation of “soft” polymer domains. Such a three-phase composite may be generated using two incompatible polymers, namely a “hard” master polymer having a distinct higher glass transition temperature compared with the second “soft” polymer. As an example, Figure 4 shows the morphologies of PDHNMA/PEMA/ZOC-1002XX composite layers formed with varying fractions of PDHNMA and PEMA which are incompatible at room temperature. The arrows in Figure 4 indicate composite domains formed by the minor polymer component, PEMA, with enclosed LC droplets.

### Indentation resistance

The mechanical stability of the composite films against external stress has been comparatively examined in three test series (I–III). Details on the samples investigated are summarized in Table IV.

In a first test run (I), type C cells were filled with mixtures prepared from ZOC-1002 XX as common LC component and five different polymers in a constant mixing ratio. Figure 5 presents polarizing optical micrographs of the resulting composite layers at room temperature indicating similar cellular textures for all samples.

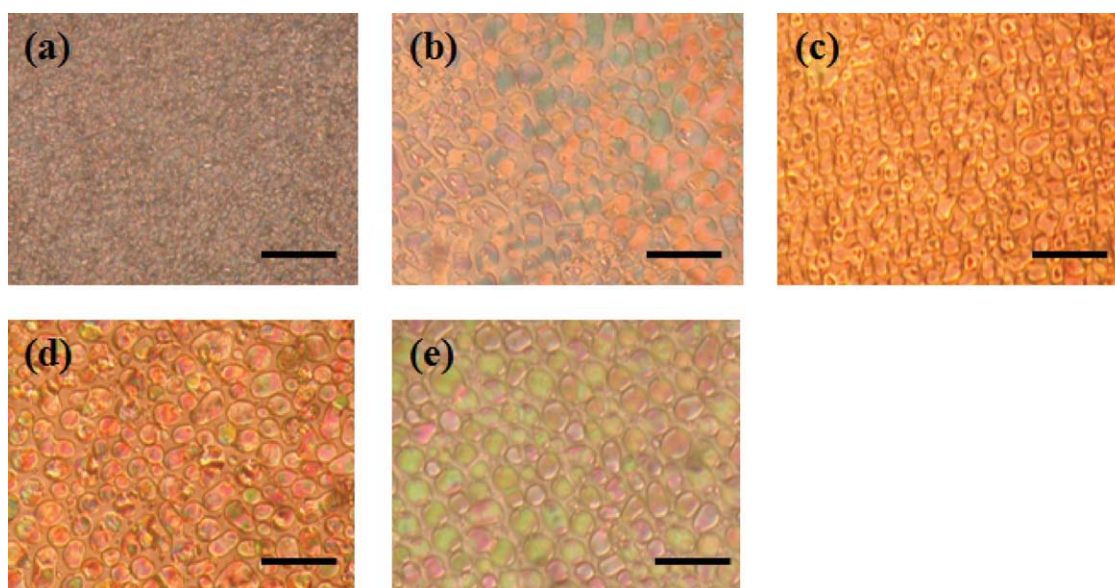
Hence, further studies were performed to achieve a ranking of the polymers with regard to their suitability to form composites offering a resistance against external stress as high as possible. For that purpose, the extension of damaged areas around an indenter head resulting from increasing indentation

was measured. As an example, in Figure 6(a,e), the sample regions of different damage at an indentation depth of 10  $\mu\text{m}$  and a cell loading of 0.3N are illustrated by different colors as described previously. In the same way, Figure 6(f–j) shows the samples at a loading of about 0.7N and an indentation depth of 30  $\mu\text{m}$ . It is obvious that the composite layers formed by PTMA [Fig. 6 (e,j)] and PTBCHMA [Fig. 6 (c,h)] offer the largest resistance against external stress. As expected, the low  $T_g$  polymer PEMA provided the smallest stabilization effect [Fig. 6 (a,f)]. No further correlation between  $T_g$  and indentation resistance could be observed.

In the test run (II), the morphology and compliance was investigated using ZOC-1002 XX containing increasing amounts of PTMA (samples II/1–II/3, I/5). Figure 7(a–d) depicts optical micrographs for four films of different compositions recorded at room temperature. Sample II/1 with low PTMA content shows large LC areas with rambling polymer walls, whereas samples with higher polymer content form isolated LC-rich compartments surrounded by a coherent polymer matrix. The average droplet size

**TABLE IV**  
Composition Data of Samples Used for Indentation Tests

Sample code	Composition (wt %)		Cell type
	LC mixture	Polymer	
I/1	ZOC-1002 XX (80)	PEMA (20)	C
I/2		PCHMA (20)	
I/3		PTBCHMA (20)	
I/4		PDHNMA (20)	
I/5		PTMA (20)	
II/1	ZOC-1002 XX (95.1)	PTMA (4.9)	C
II/2	ZOC-1002 XX (89.9)	PTMA (10.1)	
II/3	ZOC-1002 XX (86)	PTMA (14.0)	
III/1	E7 (80)	PTMA (20)	C
III/2	MDA-00-1795 (80)		
III/3	MLC-6650 (80)		

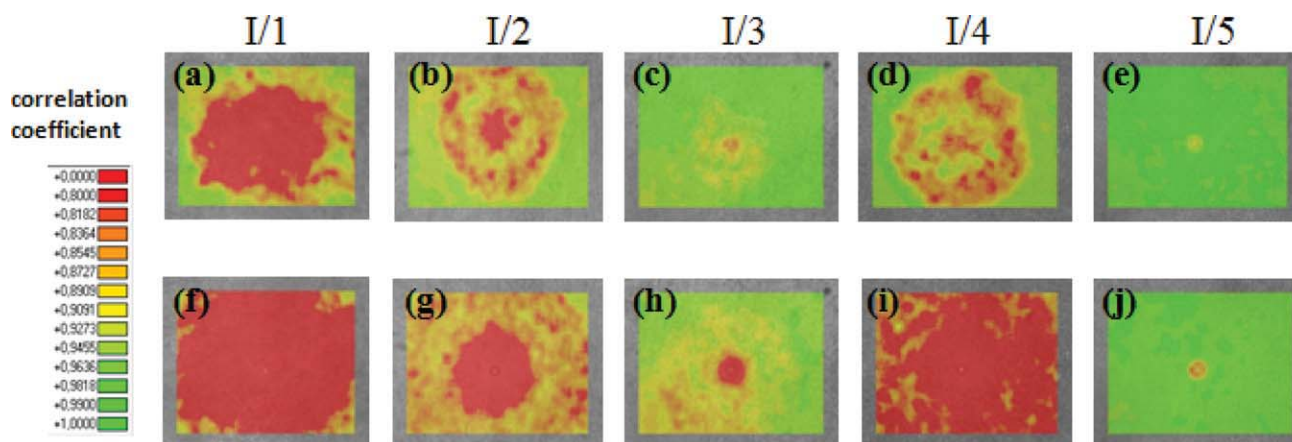


**Figure 5** Cellular textures (POM images) of composite films in type C cells containing 80 wt % ZOC-1002XX as common LC component and (a) PEMA, (b) PCHMA, (c) PTBCHMA, (d) PDHNMA, and (e) PTMA after cooling from 120°C to room temperature with 1 K/min. The lateral dimension of the LC-filled compartments in (b)–(d) is  $\sim 10 \mu\text{m}$ . Scale bars indicate 25  $\mu\text{m}$ . [Color figure can be viewed in the online issue, which is available at [www.interscience.wiley.com](http://www.interscience.wiley.com).]

decreases from about 100  $\mu\text{m}$  to 30  $\mu\text{m}$  with increasing polymer fraction. In Figure 7(e–h), the impairment of the samples after a loading of 1.2N and an indentation depth of 50  $\mu\text{m}$  are illustrated by means of the *uniDAC* method. Figure 7(i) shows the sample deformation of I/5 at a loading of 4N and an indentation depth of 178  $\mu\text{m}$ .

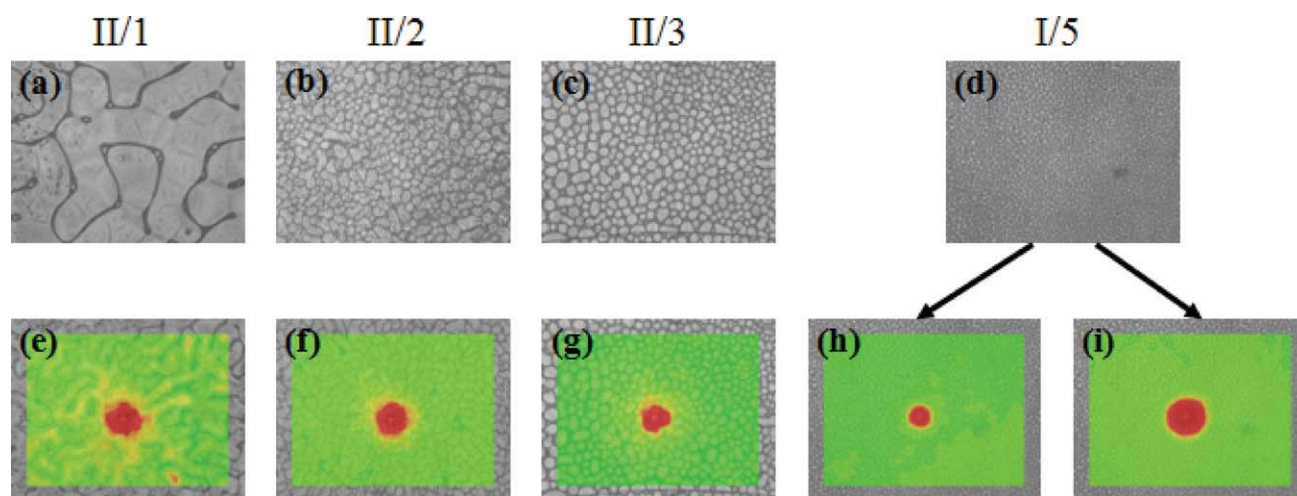
Obviously, a PTMA content of about 20 wt % seems to be an optimum. Higher polymer fractions may result in parasitic light scattering of the composite layers.

A further test run (III) was carried out with composites containing about 80 wt % of several commercial nematic LC mixtures, especially those exhibiting relatively high clearing temperatures (MDA-00-1795:  $T_{\text{ni}} = 100^\circ\text{C}$ ; MLC-6650:  $T_{\text{ni}} = 90^\circ\text{C}$ ) and PTMA (samples III/1–III/3, I/5). The results obtained for a loading of 1.2N and an indentation depth of 50  $\mu\text{m}$  are given in Figure 8(a–d). Under these conditions, the effective range of deformation by indentation loading depends only weakly on the LC mixture under study.



**Figure 6** Damaged areas in ZOC-1002 XX/polymer films (samples I/1–I/5) as revealed by the correlation coefficient. Series (a)–(e): An indentation depth of 10  $\mu\text{m}$  leading to a cell loading of 0.3N. Series (f)–(j): Damaged areas at an indentation depth of 30  $\mu\text{m}$  and a cell loading of 0.7N. Image area: 2.7 mm  $\times$  2 mm. [Color figure can be viewed in the online issue, which is available at [www.interscience.wiley.com](http://www.interscience.wiley.com).]





**Figure 7** Damaged areas in ZOC-1002 XX/PTMA films (samples II/1–II/3, I/5) as revealed by the correlation coefficient. Series (a)–(d): Microscope images of textures formed in the composite films. Series (e)–(h): Damaged areas at an indentation depth of 50  $\mu\text{m}$  and a cell loading of about 1.2*N*. (i) displays the perturbation of the sample I/5 caused by 4*N* cell loading at an indentation depth of 178  $\mu\text{m}$ . Image area: 2.7 mm  $\times$  2 mm, color scale as in Figure 6. [Color figure can be viewed in the online issue, which is available at [www.interscience.wiley.com](http://www.interscience.wiley.com).]

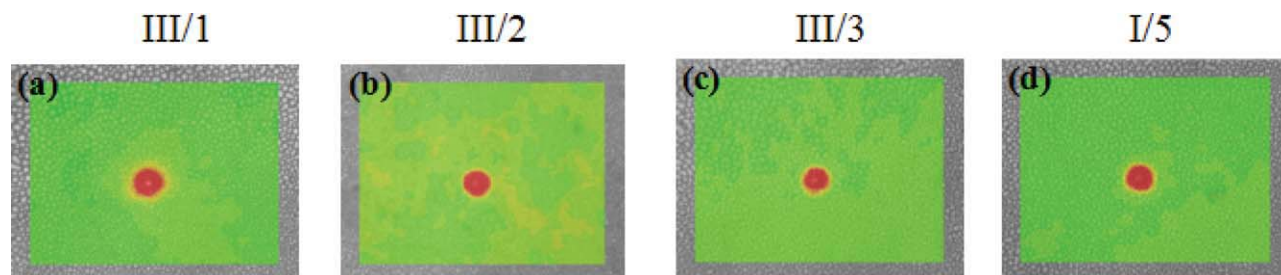
## CONCLUSIONS

It has been demonstrated that certain poly(alkyl methacrylates) and poly(cycloalkyl methacrylates) and conventional LC mixtures are well applicable for a solvent-free fabrication of polymer/LC composite layers which prevent material flow and mixing of neighboring LC domains under a typical external stress. These properties are of particular importance in view of an increasing demand to substitute rigid glass plates by flexible substrates in display construction.

Polymer/LC composite films in different cell types have been prepared by TIPS and have subsequently been subjected to indentation tests. The unstressed composites consist of oblate LC domains in the range of 5–20  $\mu\text{m}$  surrounded by coherent polymer walls. Damages resulting from indentation were

evaluated by means of the *uniDAC* image correlation method. It turned out that poly(1-tetralyl methacrylate) and poly(4-*tert*-butylcyclohexyl methacrylate) shall be used for composite formulations with respect to optimal miscibility, adequate phase separation behavior, and high indentation resistance. Furthermore, copolymers or binary blends of “hard” and “soft” polymers may offer the advantages of multi-degree-of-freedom systems. For composites formed with poly(1-tetralyl methacrylate), no significant dependence of the indentation resistance on various LC mixtures was found under the specified test conditions.

The dependence of composite properties on the compartment size distribution as well as the influence of patterned substrate surfaces on the film morphology will be the subject of future investigations.



**Figure 8** Damaged areas in LC/PTMA layers (samples III/1–III/3, I/5) at an indentation depth of 50  $\mu\text{m}$  and a loading of about 1.2*N* as revealed by the correlation coefficient. The LC components are (a) E7, (b) MDA-00-1795, (c) MLC-6650, and (d) ZOC-1002 XX. Image area: 2.7 mm  $\times$  2 mm, color scale as in Figure 6. [Color figure can be viewed in the online issue, which is available at [www.interscience.wiley.com](http://www.interscience.wiley.com).]

The authors are thankful to W. Weissflog (University Halle-Wittenberg/Germany) for many useful discussions and to Chisso Co., Tokyo/ Japan, for supply of LC mixtures.

## References

1. Ahn, W.; Kim, Y.; Kim, H.; Kim, S. C. *Macromolecules* 1992, 25, 5002.
2. Pracella, M.; Bresci, B.; Nicolardi, C. *Liq Cryst* 1993, 14, 881.
3. Ballauff, M. *Mol Cryst Liq Cryst* 1986, 136, 175.
4. De Bougrenet De La Tonnaye, J. L. *Liq Cryst* 2004, 31, 241.
5. Drzaic, P. S. *Liquid Crystal Dispersions*; World Scientific: Singapore, 1995.
6. Crawford, G. P.; Žumer, S., Eds. *Liquid Crystals in Complex Geometries Formed by Polymer and Porous Networks*; Taylor & Francis: London, Bristol, 1996.
7. Craighead, H. G.; Cheng, J.; Hackwood, S. *Appl Phys Lett* 1982, 40, 22.
8. Doane, J. W.; Vaz, N. A.; Wu, B.-G.; Žumer, S. *Appl Phys Lett* 1986, 48, 269.
9. Chang, S. J.; Lin, C. M.; Fuh, A. Y. G. *Liq Cryst* 1996, 21, 19.
10. Shiyonovskaya, I.; Green, S.; Khan, A.; Magyar, G.; Pishnyak, O.; Doane, W. J. *J Soc Inf Disp* 2008, 16, 113.
11. Chari, K.; Kowalczyk, J.; Rankin, C. M.; Johnson, D. M.; Blanton, T. N.; Capurso, R. G. *Digest of Technical Papers—Society for Information Display International Symposium, 2006, San Francisco, CA, USA*, 37, p 1741.
12. Lee, Y.-J.; Jang, S.-J.; Jung, J.-W.; Kim, H.-R.; Jin, M. Y.; Choi, Y.; Kim, J.-H. *Mol Cryst Liq Cryst* 2006, 458, 81.
13. Kim, Y.; Francl, J.; Taheri, B.; West, J. L. *Appl Phys Lett* 1998, 72, 2253.
14. Murashige, T.; Fujikake, H.; Sato, H.; Kikuchi, H.; Kurita, T.; Sato, F. *Jpn J Appl Phys* 2004, 43, L1578.
15. Yang, D.-K.; Lu, Z. J.; Chien, L. C.; Doane, J. W. *Digest of Technical Papers—Society for Information Display International Symposium, 2003, Baltimore, MD, USA*, 34, p 959.
16. Crooker, P. P.; Yang, D. K. *Appl Phys Lett* 1990, 57, 2529.
17. Kim, W.-K.; Kyu, T. *Mol Cryst Liq Cryst* 1994, 250, 131.
18. Kyu, T.; Shen, C.; Chiu, H.-W. *Mol Cryst Liq Cryst* 1996, 287, 27.
19. Carpaneto, L.; Ristagno, A.; Stagnaro, P.; Valenti, B. *Mol Cryst Liq Cryst* 1996, 290, 213.
20. Deshmukh, R. R.; Malik, M. K. *J Appl Polym Sci* 2008, 109, 627.
21. Deshmukh, R. R.; Malik, M. K. *J Appl Polym Sci* 2008, 108, 3063.
22. Bouchaour, T.; Benmouna, F.; Leclercq, L.; Ewen, B.; Coqueret, X.; Benmouna, M.; Maschke, U. *Liq Cryst* 2000, 27, 413.
23. Chen, L. G.; Shanks, R. *Liq Cryst* 2007, 34, 1349.
24. Cypcar, C. C.; Camelio, P.; Lazzeri, V.; Mathias, L. J.; Waegell, B. *Macromolecules* 1996, 29, 8954.
25. Matsumoto, A.; Mizuta, K.; Otsu, T. *J Polym Sci Part A: Polym Chem* 1993, 31, 2531.
26. Dost, M.; Vogel, D.; Winkler, T.; Vogel, J.; Erb, R.; Kieselstein, E.; Michel, B. *Proc SPIE* 2003, 5048, 73.
27. Dost, M.; Seiler, B. *Micromaterials and Nanomaterials*; Fraunhofer IZM: Berlin/Germany, 2008; Vol. 8, p 130.